International Journal on Science and Technology

One Day National Seminar on

"Advances in Life Sciences for Diversity, Applications, and Human Welfare"

(ALSDAHW – 2025)

Organized by Department of Microbiology & Department of Biotechnology

M.V.S. Government Arts & Science College (Autonomous), Mahabubnagar-509001

E-ISSN: 2229-7677 ● Website: www.ijsat.org ● Email: editor@ijsat.org

Microwave-Assisted Green Synthesis of *Punica granatum* Peel–Mediated Silver Nanoparticles with Potent Antibiofilm Activity

Ruqya Banu[1], D. Narmada[2]

[1,2]Department of Chemistry, Dr. BRR GDC Jadcherla ,Mahabubnagar Telangana, India-509301,

Abstract

Silver nanoparticles (AgNPs) were successfully synthesized using *Punica granatum* peel extract via a microwave-assisted biogenic method. This green synthesis approach is rapid, cost-effective, and environmentally friendly, avoiding toxic chemicals and harsh reaction conditions. Formation of AgNPs was confirmed by a visible color change and a characteristic surface plasmon resonance (SPR) peak at 410–430 nm in UV–Visible spectra. Synthesis parameters, including microwave irradiation time and reactant concentrations, were optimized to enhance nanoparticle yield and stability. Characterization using UV–Vis, FTIR, DLS, XRD, TEM exposed well-dispersed, spherical AgNPs with an average size of 8 ± 2nm, a low polydispersity index (0.224), and a zeta potential of −30.5mV, indicating good colloidal stability. Phytochemicals in peel extract acted as reducing as well as stabilizing agents. The synthesized AgNPs exhibited significant antibiofilm activity, highlighting their potential for biomedical and antimicrobial applications.

1. INTRODUCTION

Recently, Nanomaterials' exceptional characteristics have created a lot of attention in science and technology. They exhibit a wide range of physical, chemical, optical, mechanical, catalytic, electrical, and thermal characteristics, which make them highly valuable for numerous applications (1–6). Among these materials, metal nanoparticles have gained substantial attention over previous decade due to their nanoscale dimensions, high surface-to-volume ratio, or distinctive properties, including distinctive optical and electronic behavior, sensing capability, catalytic activity, and antibacterial effects (7–10).

In particular, AgNPs are among most extensively studied metal nanoparticles because of their broad applicability in sensors, optoelectronic devices, renewable energy systems, environmental remediation, and medical technologies (11,12). AgNPs are especially recognized for their excellent chemical stability, high catalytic efficiency, and strong antimicrobial activity (13).

Numerous techniques were developed for the synthesis of AgNPs, including thermal decomposition in organic solvents, microemulsion techniques, ultrasonic-assisted reduction, photoreduction, and biological

approaches (14). However, many conventional synthesis methods are costly, time-consuming, involve the usage of toxic chemicals that pose significant environmental as well as health risks. Additionally, these processes often generate hazardous byproducts, leading to concerns regarding environmental pollution and human safety (15). As a result, Cost-effective, sustainable, and eco-friendly nanoparticle synthesis methods are in demand(16).

Green synthesis was emerged as a promising and sustainable method, utilizing biological resources to reduce metal ions into nanoparticles. This method commonly employs microorganisms or plant-derived extracts from fruits, leaves, and seeds, which are rich in phytochemicals, namely amino acids, polysaccharides, tannins, proteins, polyphenols, ascorbic acid, enzymes, terpenoids, and flavonoids. These biomolecules function as natural capping, reducing, and stabilizing agents, while also enhancing functional properties of the synthesized nanoparticles (17–22).

In the current research, extracts from *Punica granatum* peels were used to create AgNPs. A simple and efficient green synthesis route was developed by optimizing the concentrations of *Punica granatum* peel extract and $AgNO_3$, as well as the microwave irradiation time. The synthesized AgNPs were subsequently evaluated for their antibiofilm activity. This eco-friendly synthesis strategy presents promising potential for applications in environmental remediation, dye sensing, disease treatment, particularly against drug-resistant microbial strains.

2. EXPERIMENTS

2.1 Materials

In Mahbubnagar, Telangana, India, fresh pomegranates (*Punica granatum*) were purchased from a local market. Congo red dye, crystal violet and silver nitrate (AgNO3) have been acquired from S. D. Fine Chemicals in Mumbai, India. Every chemical utilized in this investigation was analytical grade or didn't require any further processing.

2.2 Preparation of *Punica granatum* peel extract solution

The standard procedure described in the earlier study [23] was followed in production of the extract. First, double-distilled water (DDW) was used to thoroughly wash the fruits multiple times. The peel was removed gently after washing and left to fully dry at room temperature. It was ground into a fine powder after drying. After 30 minutes at 60 °C, 0.4 grams of this powder were extracted using 100ml of DDW. The mixture was filtered through Whatman filter paper for the aqueous extract.

2.3 Synthesis of silver nanoparticles

AgNO3 solution (3mL) was mixed with PG fruit peel extract solution (4mL) at different concentrations. After that, this mixture has been exposed to 650W of microwave radiation for four minutes. The reaction mixture turned yellowish-brown, demonstrating synthesis of AgNPs. The solution has then been centrifuged to eliminate any excess molecules and unreacted ions attached to AgNPs [24, 25].

2.4 Antibiofilm Studies

The antibiofilm activity of biosynthesized AgNPs has been assessed utilizing the Congo red assay, which detects biofilm formation based on Congo red binding to bacterial exopolysaccharides(26). Red colonies

indicate biofilm inhibition, while black colonies signify active biofilm formation(27). *Bacillus cereus* and *Klebsiella pneumoniae* treated with AgNPs showed red colonies, demonstrating reduced biofilm formation, whereas untreated controls displayed black colonies(28). These results are consistent with previous studies reporting effective biofilm inhibition by biosynthesized AgNPs.

2.5 Characterization techniques

The crystal structure and phase purity of as-prepared samples were examined by powder X-ray diffraction (XRD) utilizing a Rigaku Miniflex 600 X-ray diffractometer with Cu-Kα radiation (λ = 0.15406nm) over a 2θ range of 10–80°. A UV–visible spectrophotometer (UV-2600, Shimadzu) was used for optical absorption investigations. To determine functional groups and bonding interactions, the samples' "Fourier transform infrared (FTIR)" spectra have been recorded utilizing a Shimadzu IR Prestige-21 spectrophotometer. Transmission electron microscopy (TEM) was employed to analyze size as well as shape of produced products using a JEOL JEM 2100 running at a 200kV accelerating voltage. Additionally, Dynamic light scattering(DLS) has been employed to assess the nanoparticles' zeta potential (DLS; Malvern Instruments Ltd., Malvern, UK).

3. RESULTS AND DISCUSSION

Punica granatum (PG) aqueous peel extract was used in this study as a reducing and stabilizing agent in the microwave-assisted green synthesis of AgNPs. As active reaction centers that aid in the reduction of Ag^{+} to Ag^{0}, *Punica granatum*'s abundant phytochemical content also acts as a capping and stabilizing agent for the biosynthesized AgNPs. A brown coloration was seen when the PG peel extract and $AgNO_3$ solution were mixed; this indicates the creation of AgNPs, which is consistent with their surface plasmon resonance (SPR) characteristics [22,33]. Additionally, a systematic evaluation of the effects of reaction time, $AgNO_3$ concentration, and *Punica granatum* peel concentration on AgNP production was conducted. The synthesized AgNPs demonstrated strong antibiofilm activity, highlighting their potential for antimicrobial applications

3.1 UV-Visible

UV-visible absorption spectroscopy was main method employed to monitor production of AgNPs. UV–Vis absorption spectrum of as-synthesised AgNPs is illustrated in Fig. 1 and illustrates a distinctive maximum absorption in 400–420nm region, which corresponds to AgNPs' SPR band. While maintaining a constant $AgNO_3$ concentration and reaction time, various extract concentrations (0.1–0.7%) were examined to investigate the impact of *Punica granatum* (PG) peel extract concentration on AgNP production. As illustrated in Figure 1a, the SPR peak intensity increases as the peel extract concentration increases from 0.1-0.6%, suggesting a greater production of AgNPs. However, a slight decrease in peak intensity was observed at 0.7% extract concentration, suggesting that 0.6% is the optimal concentration for efficient AgNP synthesis.

Furthermore, the effect of $AgNO_3$ concentration on AgNP formation was evaluated by varying $AgNO_3$ concentration while maintaining constant extract concentration and reaction time. The corresponding UV–Vis absorption spectra are shown in Figure 1b. The SPR peak intensity increased steadily as the $AgNO_3$

International Journal on Science and Technology
One Day National Seminar on
"Advances in Life Sciences for Diversity, Applications, and Human Welfare"
(ALSDAHW – 2025)
Organized by Department of Microbiology & Department of Biotechnology
M.V.S. Government Arts & Science College (Autonomous), Mahabubnagar-509001
E-ISSN: 2229-7677 • Website: www.ijsat.org • Email: editor@ijsat.org

concentration was raised from 0.1 to 1 mM, beyond which only marginal changes were observed. This trend indicates that higher availability of Ag^+ ions in reaction mixture favors AgNP formation under optimized synthesis conditions.

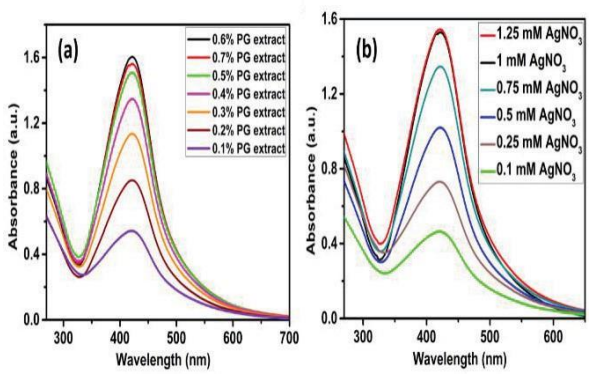

FIGURE 1. "UV-Vis absorption spectra of AgNPs synthesized with different percentages of PG extract (a) , different concentrations of $AgNO_3$ solution (b).

UV–visible absorption spectra of AgNPs synthesized under diverse microwave irradiation times are shown in Figure 2. The duration of microwave irradiation plays a crucial role in AgNP formation. As illustrated in Figure 2, a weak and broad SPR band has been noted after 1 minute of irradiation, indicating limited AgNP synthesis. The intensity of SPR peak improved gradually with increasing irradiation time up to 5minutes, beyond which no significant change was observed. These results indicate that the optimal conditions for producing homogeneous AgNPs are a 0.6% extract concentration, 1mM $AgNO_3$ concentration, and 5minutes of microwave irradiation".

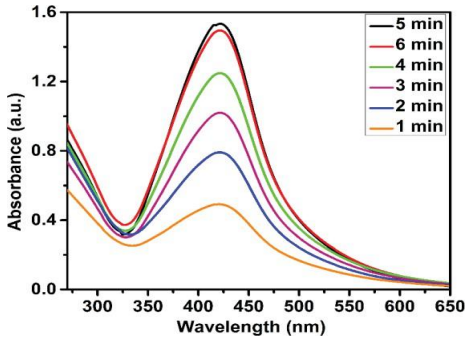

FIGURE 2. UV-Vis absorption spectra of AgNPs synthesized at varying microwave irradiation times

3.2 FTIR

The biomolecules responsible for the reduction of Ag^+ ions to AgNPs by the PG fruit peel extract have been identified using FTIR analysis. The significant absorption band between 3200 and 3500 cm^{-1} in Fig. 3 indicates O–H stretching vibrations of phenolic groups.The extract's aromatic C=C stretching vibrations

International Journal on Science and Technology
One Day National Seminar on
"Advances in Life Sciences for Diversity, Applications, and Human Welfare"
(ALSDAHW – 2025)
Organized by Department of Microbiology & Department of Biotechnology
M.V.S. Government Arts & Science College (Autonomous), Mahabubnagar-509001
E-ISSN: 2229-7677 • Website: www.ijsat.org • Email: editor@ijsat.org

cause peaks at 1726, 1610, and 1442 cm^{-1} [23, 26]. The absorption band at 2920cm^{-1} is associated with "alkyl C–H stretching vibrations. Peaks appearing at 1452,1379,1332cm^{-1} have been assigned to C–O–O stretching vibrations, while those at 1142 and 1020cm^{-1} correspond to C–C stretching vibrations. Additionally, the band at 794cm^{-1} is attributed to acetylenic C–H bending vibrations" [27–29]. Compared with "FTIR spectrum of the PG peel extract, the PG-capped AgNPs" exhibited changes in peak intensities, with some bands increasing and others decreasing. These variations suggest that functional groups exist in PG peel extract participate in reduction process and contribute to the stabilization of synthesized AgNPs.

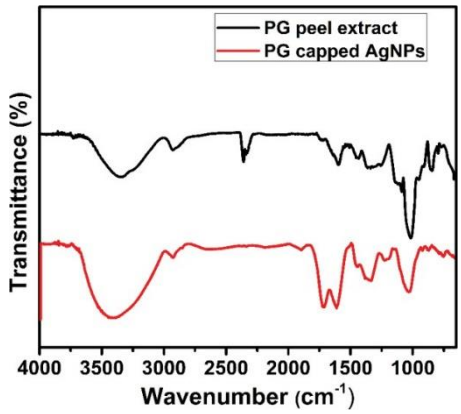

FIGURE 3. FTIR spectra of the PG peel extract and the AgNPs capped with PG peel extract were analyzed.

3.3 XRD

"The lattice and crystalline structure of the produced AgNPs were examined using XRD. Figure 4 shows the ideal AgNPs XRD pattern. AgNPs' face-centered cubic (FCC) structure has distinct diffraction peaks at 38.33°, 44.28°, 64.42°, and 77.60°, corresponding to the (111), (200), (220), and (311) crystallographic planes". The good agreement between these diffraction peaks and the standard JCPDS file confirms the successful creation of crystalline AgNPs. 42-0783 [30]. These findings are consistent with past reports in the literature [31].

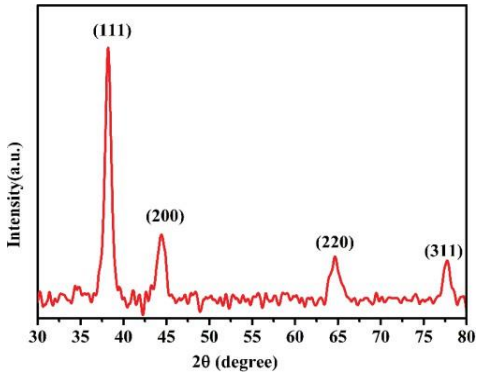

FIGURE 4. The "XRD pattern of AgNPs capped with PG peel extract was examined.

International Journal on Science and Technology
One Day National Seminar on
"Advances in Life Sciences for Diversity, Applications, and Human Welfare"
(ALSDAHW – 2025)
Organized by Department of Microbiology & Department of Biotechnology
M.V.S. Government Arts & Science College (Autonomous), Mahabubnagar-509001
E-ISSN: 2229-7677 • Website: www.ijsat.org • Email: editor@ijsat.org

3.4 TEM

Figure 5 presents TEM analysis of AgNPs under optimal conditions". TEM pictures show that synthesized AgNPs are spherical and well-monodispersed. The as-synthesized nanoparticles exhibit a very small average size of 8 ± 2 nm. Furthermore, high-resolution TEM (HRTEM) micrographs (Figure 5b) were used to examine the crystalline nature of individual nanoparticles. These pictures show distinct lattice fringes that align with previously reported findings [32, 33] and have an interplanar spacing of 0.236nm, corresponding to the silver's (111) plane.

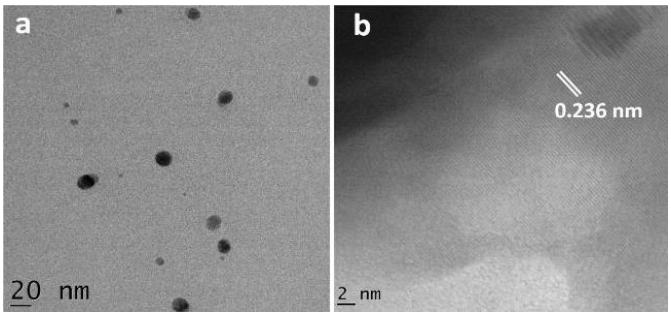

FIGURE 5 .TEM (a) and HRTEM (b) images of PG peel extract–capped AgNPs.

3.5 DLS

One of the most practical and versatile methods for figuring average particle size as well as zeta potential is DLS. The distributed AgNPs "were capped with negatively charged functional groups, indicating great stability, as indicated by a zeta potential value of −30.5mV (Fig. 6a). The average particle size of generated AgNPs was approximately 12.52nm (Fig. 6b").

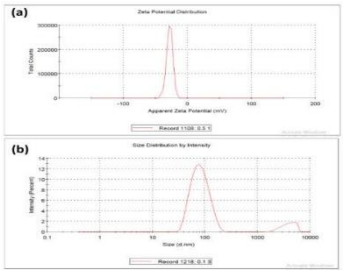

FIGURE 6. Zeta potential (a) and particle size distribution (b) of PG peel extract–capped AgNPs.

3.6 Proposed mechanism involved in the formation of silver nanoparticles

According to most previous studies, AgNPs are formed and stabilized by various phytochemicals present in plant extracts [26–29]. In this work, PG fruit peel extract was used to create AgNPs utilizing a green synthesis method. Many carboxylic, hydroxyl, and aromatic functional groups found in this extract can interact with Ag^{+} ions, convert them to Ag^{0}, and then stabilize AgNPs that are produced [23]. The use of PG fruit peel extract in various approaches for production of AgNPs has also been reported in the past.

3.7 Antibiofilm Studies

As explained by Freeman and coworkers [25], the Congo red agar (CRA) method has been employed to evaluate biofilm inhibition activity of AgNPs. "Luria-Bertani (LB)" broth has been employed to cultivate cultures of *Bacillus cereus* and *Klebsiella pneumoniae*, which were then incubated for "24h at 37 °C. A brain heart infusion (BHI) agar medium was made using 0.08% (w/v) Congo red dye and 5% (w/v) sucrose. Except Congo red, which had been sterilized separately then added to the medium at 55 °C, all medium components were autoclaved together. Distilled water was used to generate AgNP suspensions at concentrations of 5, 10, 20, 40, 80, 100µg/mL. These suspensions have then been placed across different solidified agar plates and allowed to diffuse for six to ten minutes. The bacterial strains were cultured aerobically at 37 °C for 24 hours after being streaked in two directions. Black colonies were formed by bacteria that created biofilms, while red colonies were formed by bacteria that inhibited biofilms.

To further quantify biofilm inhibition, the biosynthesized AgNPs were tested against *Bacillus cereus* and *Klebsiella pneumoniae* by utilizing a crystal violet assay. Bacterial cultures grown for 12to14h have been diluted 1:100(v/v) in fresh medium, and 200µL aliquots had been transferred to wells of a 96-well tissue culture plate (TCP), which had been incubated at 37 °C for 16 hrs without shaking. Each well was treated with 10 µL of AgNP suspension at concentrations of 100,50,25, and 12.5µg/mL. Following the measurement of the optical density at 600 nm (OD_{600}), planktonic cells were extracted, and non-adherent cells were gently washed out of wells utilizing 200µL of phosphate-buffered saline (PBS, pH 7.2). To stain adherent biofilm, 200µL of 0.1% (w/v) crystal violet solution has been added to every well of plates" after they had been air-dried for ten minutes. The plates were then incubated for ten minutes. 95% ethanol was used to dissolve the bound color after excess stain was removed with deionized water. An ELISA plate reader has been employed to quantify absorbance at 595nm, and treatment and control wells were compared to regulate percentage of biofilm inhibition. The basic controls used to measure the suppression of biofilm formation were 200 µL of ethanol and 200 µL of crystal violet.

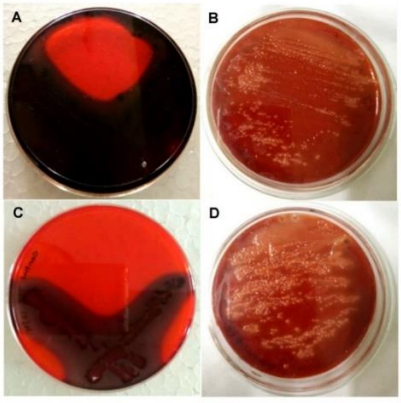

FIGURE 7 Assessment of antibiofilm activity of AgNPs by CRA plate method. Biofilm development is shown by black colonies (A, C), whereas black colony formation is suppressed by AgNP treatment. *Bacillus cereus* (A, B); *Klebsiella pneumoniae* (C, D).

Furthermore, crystal violet staining has been employed to assess biofilm inhibition efficiency of AgNPs (Figure 8). The results demonstrated that bacterial strains treated with AgNPs exhibited significantly reduced biofilm formation. This inhibition was clearly indicated by the decreased intensity of crystal violet staining in biofilm-forming bacteria (Figure 8A). The extent of biofilm inhibition increased as AgNP concentration has been raised from 12.5 to100µg/mL (Figure 8B). In addition, *Bacillus cereus* showed greater susceptibility to biofilm inhibition at higher AgNP concentrations compared to *Klebsiella pneumoniae*. Overall, these outcomes recommend that biosynthesized AgNPs effectively inhibit biofilm formation and demonstrate antibacterial activity against Gram-positive as well as Gram-negative bacterial strains.

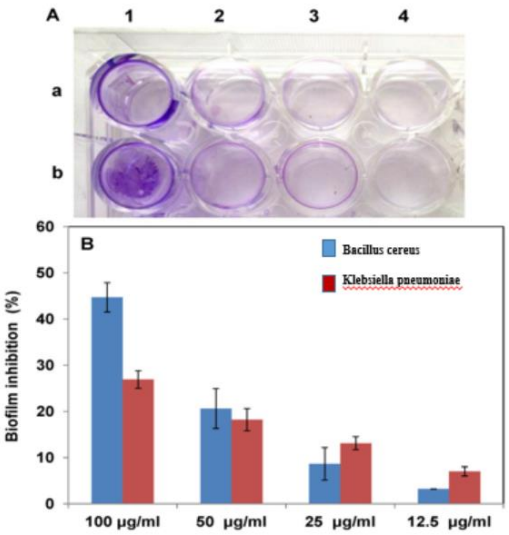

FIGURE 8. AgNPs' antibiofilm activity has been assessed using crystal violet assay. (A) *Bacillus cereus* and *Klebsiella pneumoniae* are represented by rows a and b, correspondingly, with increasing AgNPs concentrations(12.5to100µg/mL) indicated as 1-4. (B) Quantitative depiction of antibiofilm activity. The suppression of biofilms has been dose-dependent.

4. CONCLUSION

In this study, *Punica granatum* peel extract was successfully utilized as a reducing or stabilizing agent for green synthesis of AgNPs. The synthesized AgNPs exhibited a spherical morphology with a face-centered cubic crystal structure or an average particle size of 8 ± 2nm. Furthermore, the AgNPs demonstrated significant antibiofilm activity, indicating their potential application in textiles, food packaging, sensing devices, biomaterials, water purification systems. Owing to their strong antimicrobial properties, these nanoparticles may also be promising candidates for biomedical applications, including wound dressings and catheter coatings.

ACKNOWLEDGMENT

The infrastructure facilities required to carry out the experiments were provided by Palamuru University's Department of Chemistry, for which the authors are grateful. Additionally, the authors thank Osmania University's Department of Chemistry to provide other necessary facilities. Additionally, the authors would like to thank Prof. G. Sukanya, Principal of "Dr. B.R.R. Government Degree College, Jadcherla," to provide the essential facilities and support.

REFERENCES

1. Diksha J, Prasanna Kumar T, Rajiv P, Bipul Kumar, Hemant K.Gautam, Shrish Agnihotri, Ashwani Kumar Sharma, and Pradeep Kumar, Mater. Sci. Eng. C,**80**, 659-669 (2017).
2. Daniel M. C. and Astruc D., Chem. Rev., **104**, 293-346 (2004).
3. Roduner E., Chem. Soc. Rev., **35**, 583-592 (2006).
4. GuoJ. Z., Cui H., Zhou W., and Wang W., J. Photochem. Photobiol. A,**193**, 89-96 (2008).
5. Huang C.C., Yang Z., Lee K.H., and Chang H.T., Angew. Chem. Inter. Edit., **46**, 6824-6828 (2007).
6. Peto G., Molnar G. L., Paszti Z., Geszti O., Beck A., and Guczi L., Mater. Sci. Eng. C, **19**, 95-99 (2002).
7. Ostuni E, Chen C.S, Ingber D. E, and Whitesides G.M, Langmuir, **17**, 2828-2834 (2001).
8. Joannopoulos J.D, Johnson S.G, Winn J. N, and Meade R.D., NJ: Princeton University Press; (2008).
9. Guo X, Baumgarten M, and Müllen K. ProgPolymSci, **38**, 1832-1908 (2013).
10. Arinstein A, Burman M, Gendelman O, and Zussman E. Nat.Nanotechnol.**2**, 59-62 (2007).
11. Mashwani Z.U.R, Khan T, Khan M. A, and Nadhman A. Appl.Microbiol.Biotechnol.,99, 9923-9934. (2015)
12. Rostami-Vartooni A, Nasrollahzadeh M, and Alizadeh M.,J. Colloid.Interf. Sci.470, 268-275 (2016).
13. Hinojos-Márquez E. A, López-Esparza J, Espinosa-Cristóbal L. F, Donohue-Cornejo A, and Reyes-López S.Y. Ind. Eng. Chem. Res.,55, 12532-12538 (2016).
14. Ahmed S, Ahmad M, Swami B.L, and Ikram S., J. Adv. Res.,7, 17–28 (2016).
15. Prabhu S., and Poulose E.K., Int. Nano Lett.,2, 32 (2012).
16. Parashar U.K., Saxena P.S., and Srivastava A., J.Nanomater. Biostruct.,4, 159-166 (2009).
17. ArumaiSelvan D, Mahendiran D, Senthil Kumar R, and KalilurRahiman A., J.Photochem.Photobiol. B180, 243–252 (2018).
18. Baghayeri M, Mahdavi B, Hosseinpor-Mohsen Abadi Z, and Fardahi S. Appl. Organometal Chem.,32, 1–9 (2018). 19. Tippayawat P, Phromviyo N, Boueroy P, and Chompoosor A. Peer J.,4, 1–15 (2016).
19. Yeasmin S, Datta H.K, Chaudhuri S, Malik D, Abhijit Bandyopadhyay A.,J. Mol. Liq.,242, 757–66 (2017).
20. Vinay S.P, Chandrashekar N, Chandrappa C.P. IJEDR, 5, 1608–1613 (2017).
21. Rajeshkumar S, and Rinitha G. Open Nano 3, 18–27 (2018).
22. Jebakumar Immanuel Edison, and Sethuraman M.G., Spectrochim. Acta Part A: Mol. Biomol. Spectro.,104, 262–264 (2013).
23. Bhagavanth Reddy Gangapuram, RajkumarBandi, Madhusudhan Alle, Ramakrishna Dadigala, Girija

MangatayaruKotu, Veerabhadram Guttena, J. Mol. Struc.,1167, 305-315(2018).
24. Ruqya Banu.,G.Bhagvanth Reddy and K. Girija Mangatayaru, AJP Conference proceedings, 2269,030074(2020).
25. Tripathi D., Modi A., Narayan G., Rai S.P., Mater. Sci. Eng. C, 100, 152-164 (2019).
26. Bulut E., and Ozacar M., Ind. Eng. Chem. Res.,48, 5686–5690 (2009).
27. Johan M.R, Si-Wen K, Hawari N, and Aznan N.A.K. Int. J. Electrochem. Sci., 7, 4942-4950 (2012).
28. Pawan Kaur, Rajesh Thakur and Ashok Chaudhury, Green Chem. Lett. Rev., 9, 33-38 (2016).
29. Shanmugavadivu1 M., Selvam Kuppusamy and Ranjithkumar R., American J. Adv. Drug Delivery,2, 174-182 (2014).
30. Vanaja M., Paulkumar K., Baburaja M., Rajeshkumar S., Gnanajobitha G., Malarkodi C., Sivakavinesan M., and Annadurai G., 8 (2014)
31. Keshaw R. Aadil, Neha Pandey, Solange I.Mussatto, Harit Jha, J. Environ. Chem. Eng., 7, 103296 (2019).
32. Hui Y, Yan-yu R, Tao W, and Chuang W. Results Phys.,6, 299–304 (2016).
33. Girón-Vázqueza N.G., Gómez-Gutiérreza C.M., Soto-Roblesa C.A., Navaa O., Lugo-Medinab E., Castrejón Sánchezc V.H., Vilchis-Nestord A.R., and Luque P.A., Results in Physics 13, 102142 (2019).